Noise on resistive switching: a Fokker–Planck approach

G A Patterson[1,4], D F Grosz[2,3] and P I Fierens[1,3]

[1] Instituto Tecnológico de Buenos Aires, C1106ACD Buenos Aires, Argentina
[2] Instituto Balseiro, San Carlos de Bariloche, Argentina
[3] Consejo Nacional de Investigaciones Científicas y Técnicas, C1040AAH CABA, Argentina
E-mail: gpatters@itba.edu.ar, grosz@ib.edu.ar and pfierens@itba.edu.ar

Online at stacks.iop.org/JSTAT/2016/054043
doi:10.1088/1742-5468/2016/05/054043

Abstract. We study the effect of internal and external noise on the phenomenon of resistive switching. We consider a non-harmonic external driving signal and provide a theoretical framework to explain the observed behavior in terms of the related Fokker–Planck equations. It is found that internal noise causes an enhancement of the resistive contrast and that noise proves to be advantageous when considering short driving pulses. In the case of external noise, however, noise only has the effect of degrading the resistive contrast. Furthermore, we find a relationship between the noise amplitude and the driving signal pulsewidth that constrains the persistence of the resistive state. In particular, results suggest that strong and short driving pulses favor a longer persistence time, an observation that may find applications in the field of high-integration high-speed resistive memory devices.

Keywords: stochastic processes (theory)

[4] Current address: Departament d'Enginyeria Electrònica, Universitat Autònoma de Barcelona, Barcelona, Spain

Contents

1. Introduction

In recent years, several technologies have emerged as candidates to replace the current generation of non-volatile memories. A promising technology, known as resistive random access memories (RRAMs), relies on the storage of digital data on distinct resistive states, and is based on the phenomenon of resistive switching, i.e. the ability displayed by certain materials to switch between resistive states when subjected to an external electric field. Such behavior provides a physical realization of a memristor, first introduced by Chua [1]. The potential application of resistive switching to high-density information storage motivates the investigation of the influence of noise in such devices. Stotland and Di Ventra were the first to present an analysis of the influence of noise on memristors [2] and ensuing work by our group further explored the interplay between noise and resistive switching [3–6]. In [2], the influence of additive white Gaussian noise was studied using a simple model of a memristor put forth by Strukov *et al* [7]. By means of numerical simulations, it was shown that the contrast between low- and high-resistive states is enhanced by the addition of internal noise when a weak harmonic driving signal is applied, and an explanation of the observed phenomenon in terms of stochastic resonance was provided.

In this paper, we go back to the work by Stotland and Di Ventra and extend it in several directions. First, motivated by the application of resistive switching for RRAMs, we consider a non-harmonic (pulsed) driving signal and provide a theoretical explanation of the observed behavior in terms of the related Fokker–Planck (FP) equation. Then, we consider the case of external noise, i.e. noise added to a weak driving signal, a case of practical interest as it deals with fluctuating and/or noisy driving signals, where we also offer a qualitative understanding by resorting to the corresponding FP equation. Although we have already dealt with these problems in [3], only intuitive and incomplete explanations were provided and a deeper understanding is obtained by studying the FP

equations. We must also note that Slipko *et al* [8] have already used the FP equation to study the behavior of a memristor-capacitor circuit driven by white Gaussian noise.

2. A simple model of a memristor

Strukov *et al* [7] introduced a one-dimensional model of a memristor consisting of a sample of length L divided into two doped/undoped regions with oxygen vacancies. Each region has a resistance which depends on its doping level and the net sample resistance is computed as the resulting in-series value of both regions. Letting $z \in [0, L]$ denote the position of a well-defined boundary between the two regions, resistance is calculated as

$$R(z) = R_{\text{off}} - (R_{\text{off}} - R_{\text{on}})z/L,$$

where $R_{\text{off}} > R_{\text{on}}$. As oxygen vacancies drift under the influence of an externally applied voltage $U(t)$, the position z of the boundary moves. The motion of the boundary can be modeled by

$$\frac{\mathrm{d}z}{\mathrm{d}t} = \frac{\mu R_{\text{on}}}{L} F(z) \frac{U(t)}{R(z)},$$

where μ is the average dopant mobility. $F(z)$ is a function that serves two purposes. On the one hand, it accounts for the experimentally observed nonlinearities. On the other hand, letting $F(0) = F(L) = 0$ implicitly constrains the boundary to move in $[0, L]$. In this work, we use one of the simplest functions proposed in the literature [2, 7]: $F(z) = 1 - (2z/L - 1)^2$.

It is sometimes convenient to work with dimensionless variables. Let A be some suitable normalizing voltage. Then, defining $v = U/A$, $x = z/L$, $\delta R = (R_{\text{off}} - R_{\text{on}})/R_{\text{off}}$, and $\tau = \mu A R_{\text{on}}/(L^2 R_{\text{off}})t$, the resistance in a memristor can be written as

$$R(x) = R_{\text{off}}(1 - \delta R\ x), \tag{1}$$

and the new state variable $x \in [0, 1]$ is governed by the equation

$$\frac{\mathrm{d}x}{\mathrm{d}\tau} = \frac{4x(1-x)}{1 - \delta R\ x} v(\tau). \tag{2}$$

Integrating equation (2) we find that

$$\frac{x(\tau)}{(1 - x(\tau))^{1/\beta}} = g(\tau), \tag{3}$$

where $\beta = (1 - \delta R)^{-1}$ and

$$g(\tau) = \frac{x(0)}{(1 - x(0))^{1/\beta}} \exp\left\{ 4 \int_0^\tau v(t)\mathrm{d}t \right\}, \tag{4}$$

where we have assumed that $x(0) \neq 1$. From equation (2), it is readily seen that the solution is trivial and $x(\tau) = 1$ for all $\tau \geqslant 0$ when $x(0) = 1$. Hence, $x(\tau)$ can be found as a solution to the equation

$$x^{\beta}(\tau) + g^{\beta}(\tau)x(\tau) - g^{\beta}(\tau) = 0. \tag{5}$$

It is easy to see that in the particular case where $\beta = 2$, $x(\tau)$ can be found as the solution of a quadratic equation. In [9], Cai *et al* present an analytical study of the behavior of the state variable x. Biolek *et al* [10] also derive an explicit expression for the resistance. In our case, we only need to point out the dependence of the solution on the initial condition $x(0)$.

3. Internal noise

In this section, we consider the case in which equation (2) is modified by additive white Gaussian noise $\eta(\tau)$ such that $\langle \eta(\tau) \rangle = 0$ and $\langle \eta(\tau)\eta(\tau') \rangle = \Gamma\delta(\tau - \tau')$. We shall understand the resulting equation as an Ito stochastic differential equation (see [11]). Furthermore, we consider a non-harmonic driving voltage $v(\tau)$ consisting of a sequence of pulses of duration τ_b: $+1 \to -1 \to +1 \to \cdots$

Figure 1 shows the temporal evolution of $\langle x \rangle$ for several noise intensities, $\tau_b = 1$, and $\delta R = 3/4$. Observe that the maximum mean value of the state variable x reaches after a $+1$ pulse is applied decreases as the noise intensity increases, as noted by circles and arrows. The usual way of quantifying the contrast between low (R_l) and high (R_h) resistance states is through the electric pulse induced resistance (EPIR) ratio given by $(R_h - R_l)/R_l$. As can be observed in figure 2, for certain pulse durations, the EPIR ratio is maximized at a given noise intensity. We must note that results in figure 2 are different from those presented in [3]. The difference is due to a floating-point rounding error in the algorithm used in our previous work.

Results in figure 1 can be understood by resorting to the related FP equation

$$\frac{\partial P}{\partial \tau} = -\frac{\partial}{\partial x}\left\{ \frac{4x(1-x)}{1 - \delta R\ x} v(\tau) P(x,\tau) \right\} + \frac{\Gamma}{2}\frac{\partial^2}{\partial x^2} P(x,\tau), \tag{6}$$

where $P(x,\tau)$ is the probability density of $x(\tau)$. Assuming that τ_b is large enough, we can work with the stationary solution to this equation, i.e. $P(x,\tau_b) \approx P_s(x)$. Letting V denote the pulse amplitude, the stationary distribution can be obtained from the solution to the equation

$$\frac{\partial^2}{\partial x^2} P_s(x) = \frac{\partial}{\partial x}\left\{ \frac{2}{\Gamma}\frac{4x(1-x)}{1 - \delta R\ x} V P_s(x) \right\}. \tag{7}$$

Integrating once,

$$\frac{\partial P_s}{\partial x} - \left.\frac{\partial P_s}{\partial x}\right|_{x=0} = \frac{2}{\Gamma}\frac{4x(1-x)}{1 - \delta R\ x} V P_s(x), \tag{8}$$

where we assume that the right-hand side is zero at $x = 0$ (i.e. $\lim_{x\to 0} x P_s(x) = 0$). Since x is constrained to the interval [0, 1], the net flow of probability across its borders has to be zero. Thus, we assume reflecting barriers at 0 and 1 (see, e.g. [11]) and, hence, $\left.\frac{\partial P_s}{\partial x}\right|_{x=0} = \left.\frac{\partial P_s}{\partial x}\right|_{x=1} = 0$. We obtain

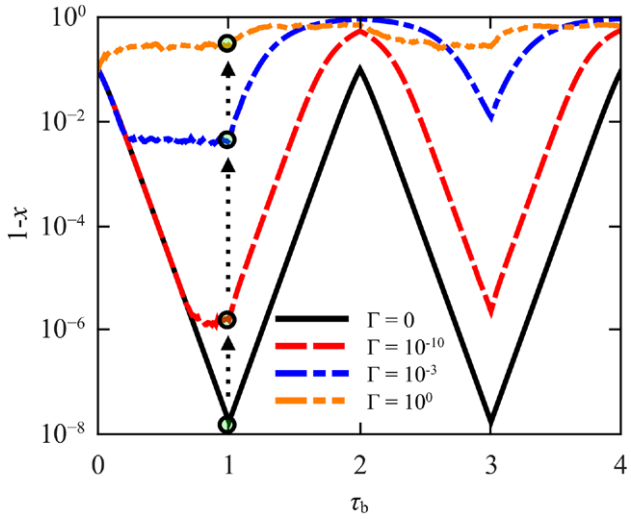

Figure 1. Temporal evolution of the state variable x for several noise intensities, $\tau_b = 1$, and $\delta R = 3/4$. Results from the average of 1000 noise realizations.

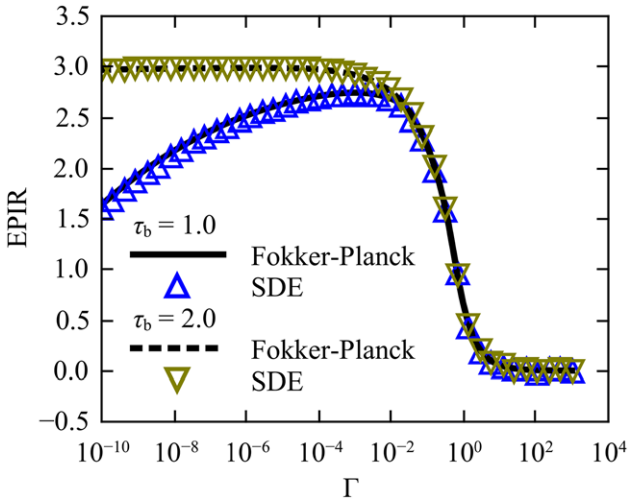

Figure 2. EPIR ratio versus internal noise intensity for $\delta R = 3/4$. Solid and dashed lines correspond to quasi-analytic predictions based on the stationary probability distribution (equation (9)) and the deterministic solution (equations (3)–(5)) for low noise intensities. Triangles: results of the average of 1000 realizations of the stochastic differential equation.

$$P_s(x) \propto \exp\left\{\frac{2}{\Gamma}\int_0^x V\frac{4y(1-y)}{1-\delta R y}\mathrm{d}y\right\}, \tag{9}$$

where $\langle x(\tau_b)\rangle$ can be computed by numerical integration. Figure 3 shows a good agreement between simulations of the stochastic differential equation and results obtained through the stationarity hypothesis. As readily seen from equations (3)–(5), the deterministic evolution of $x(\tau)$ depends strongly on the initial condition. One of the effects of noise is to erase the memory of the initial condition. Indeed, as expected, the stationary probability distribution in equation (9) does not depend on the initial condition.

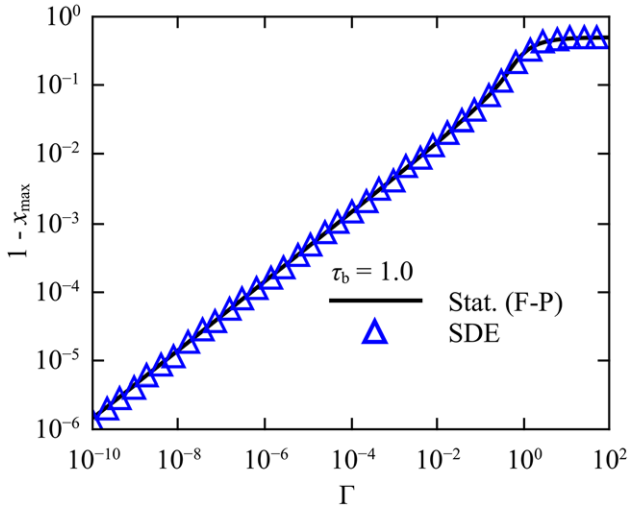

Figure 3. $x(\tau_b)$ versus noise intensity for $x(0) = 0.9$ and $\delta R = 3/4$. Approximation using the stationary distribution (solid line) and by integration of the stochastic differential equation (triangles).

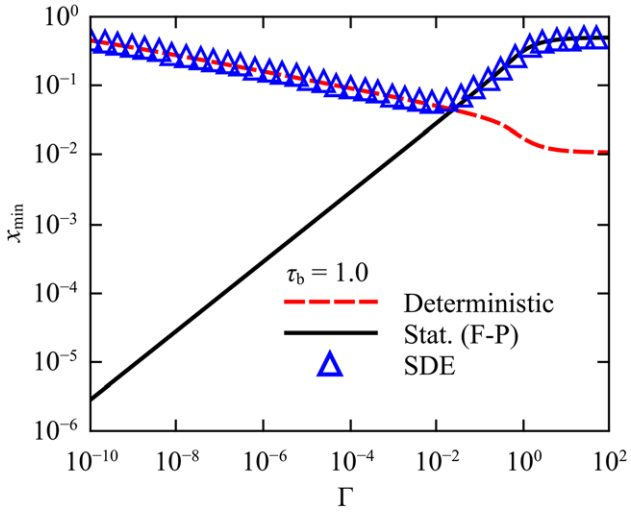

Figure 4. $x(2\tau_b)$ versus noise intensity for $x(0) = 0.9$ and $\delta R = 3/4$. Approximation using the stationary distribution (solid line), approximation using the deterministic solution (dashed), and the result of integrating the stochastic differential equation (triangles).

However, the time required to reach stationarity does depend on the initial condition (first term in equation (6)). In general, such convergence time decreases as the noise intensity increases, i.e. a higher noise intensity erases the memory of the initial condition faster.

We can try and use the stationary hypothesis to compute the minimum value attained by x after a -1 pulse is applied, i.e. $x(2\tau_b)$. Figure 4 shows $\langle x(2\tau_b)\rangle$ as a function of the noise intensity (the stationary probability is similar to that in equation (9)). The behavior for low noise intensities deviates from that predicted by the stationary distribution. Indeed, for the given initial condition ($\langle x(\tau_b)\rangle$ in figure 3, the mean value of

x at the end of the previous +1 pulse), the pulse duration τ_b is not long enough to allow for the convergence to stationarity and higher noise intensities are required to erase the memory of the initial condition. Moreover, for a low noise intensity, the value of $\langle x(2\tau_b)\rangle$ can be approximated by the deterministic solution in equations (3)–(5).

Using the predictions based on the stationary probability distribution and the deterministic solution (for low noise intensities) in figures 3–4, we can estimate the EPIR ratio. The result is shown in figure 2 and agrees very well with simulations. Intuitively, the main effect of adding noise is to lower the value of x at the end of the first +1 pulse in such a way that $\langle x(\tau_b)\rangle$ is smaller than that expected from the deterministic solution. For low noise intensities, this 'new' initial condition of the differential equation for $\tau > \tau_b$ results in a mean value of $x(2\tau_b)$ smaller than that in the noiseless case and, as such, leads to an enhanced EPIR ratio. For higher noise intensities, the values of the state variable x attained at the end of each pulse are independent of the initial conditions and determined by the stationary solution of the corresponding FP equation. Furthermore, as Γ increases the distribution in equation (9) broadens, $\langle x_s\rangle$ tends to 1/2, and the EPIR ratio approaches zero.

Let us now return to equations (8)–(9). From equation (8), it is easy to see that $P_s(x)$ is increasing (decreasing) when $V > 0$ (<0). Thus, $P_s(x)$ attains its maximum at $x = 1$ when a positive input is applied, and at $x = 0$ when the input voltage is negative. Evaluating the integral in the exponent of equation (9), we find

$$P_s(x) \propto \exp\left\{\frac{8\,V}{\Gamma}\left[\frac{\delta R x(\delta R x - 2\delta R + 2) + 2(1-\delta R)\log(1-\delta R x)}{2(\delta R)^3}\right]\right\}. \tag{10}$$

Although this expression is not complex, we can get a better insight by assuming that $\delta R \ll 1$. In this case, $\log(1-\delta R\ x) \approx -\delta R\ x$ and

$$P_s(x) \approx \mathcal{N}\exp\left\{\frac{x^2}{\frac{\Gamma\delta R}{4\,V}}\right\}, \tag{11}$$

where $\mathcal{N}$ is a normalizing constant. From this expression, it is easy to see that the stationary distribution is almost uniform when $\frac{\Gamma\delta R}{4|V|} \gg 1$, and that it peaks at the extremes of the interval when $\frac{\Gamma\delta R}{4|V|} \ll 1$. Although one may expect the dispersion of the distribution to depend on the ratio $\Gamma/|V|$, we find the influence of δR to be nontrivial. Indeed, it is as if the noise intensity, measured by Γ, is effectively scaled by δR. Since δR is a measure of the highest possible contrast between the low- and high-resistance states of the memristor, we must conclude that a higher contrast leads to a higher uncertainty on the resistance attained under the influence of internal noise. Equation (11) allows us to compute approximations to the stationary mean value of x,

$$\langle x_s\rangle \approx \mathcal{N}\frac{\Gamma\delta R}{8\,V}\left[\exp\left\{\frac{4\,V}{\Gamma\delta R}\right\} - 1\right]. \tag{12}$$

Using this result together with equation (1), we can estimate the EPIR ratio when the stationary hypothesis holds

$$\langle \text{EPIR} \rangle \approx \frac{R(\langle x_s^- \rangle) - R(\langle x_s^+ \rangle)}{R(\langle x_s^+ \rangle)} = \delta R \frac{\langle x_s^+ \rangle - \langle x_s^- \rangle}{1 - \delta R \langle x_s^+ \rangle}$$
$$\approx \frac{\Gamma \delta R^2}{8|V|} \frac{\mathcal{N}^+ \mathrm{e}^{\frac{4|V|}{\Gamma \delta R}} + \mathcal{N}^- \mathrm{e}^{-\frac{4|V|}{\Gamma \delta R}} - \mathcal{N}^+ - \mathcal{N}^-}{1 - \frac{\mathcal{N}^+ \Gamma \delta R^2}{8|V|} \left[\mathrm{e}^{\frac{4|V|}{\Gamma \delta R}} - 1 \right]},$$

where the superscript $+$ $(-)$ denotes the stationary values when the input voltage is positive (negative). In the limit of large noise, $\mathcal{N}^+ \approx \mathcal{N}^- \approx 1$. Moreover, when $\frac{\Gamma \delta R}{4|V|} \gg 1$,

$$\langle \text{EPIR} \rangle \approx \frac{\Gamma \delta R^2}{8|V|} \frac{\left(\frac{4|V|}{\Gamma \delta R}\right)^2}{1 - \frac{\Gamma \delta R^2}{8|V|} \frac{4|V|}{\Gamma \delta R}} = \frac{2|V|}{\Gamma \left(1 - \frac{\delta R}{2}\right)} \approx \frac{2|V|}{\Gamma}. \tag{13}$$

As expected, the EPIR ratio decreases with increasing noise intensity. This behavior agrees qualitatively with results shown in figure 2. For a low noise intensity and $\frac{\Gamma \delta R}{4|V|} \ll 1$, $\langle x^+ \rangle \approx 1$, $\langle x^- \rangle \approx 0$ and, hence, $\langle \text{EPIR} \rangle \approx \delta R/(1 - \delta R)$. It is readily seen that this is the value observed in figure 2 for small Γ and $\tau_b = 2$.

Let us now consider the opposite case where $\delta R \approx 1$. Letting $\delta R = 1$ in equation (9), it is easy to see that

$$P_s(x) \approx \mathcal{N} \exp\left\{ \frac{x^2}{\frac{\Gamma}{4V}} \right\}. \tag{14}$$

Therefore, equations derived for $\delta R \ll 1$ are also valid in this case if we simply substitute $\delta R = 1$.

Summarizing, whenever the pulse length τ_b is long enough in order to assume that that stationary distributions are reached, no gain in the EPIR ratio can be obtained. However, if τ_b is shorter (e.g. $\tau_b = 1$ in figure 2), then there is an optimal noise intensity for which the EPIR ratio is maximized. As such, from an application point of view, internal noise may be advantageously used to make faster memory devices based on resistive switching.

4. External noise

In this section we consider the case of external noise, i.e. the case in which the state variable x is governed by the equation

$$\frac{\mathrm{d}x}{\mathrm{d}\tau} = \frac{4x(1-x)}{1 - \delta R\ x} (v(\tau) + \eta(\tau)), \tag{15}$$

where $\eta(\tau)$ is white Gaussian noise as before. Figure 5 shows the mean EPIR ratio as a function of noise intensity for several pulse widths ($x(0) = 0.9$). It is observed that there is no optimal noise intensity that maximizes the EPIR ratio.

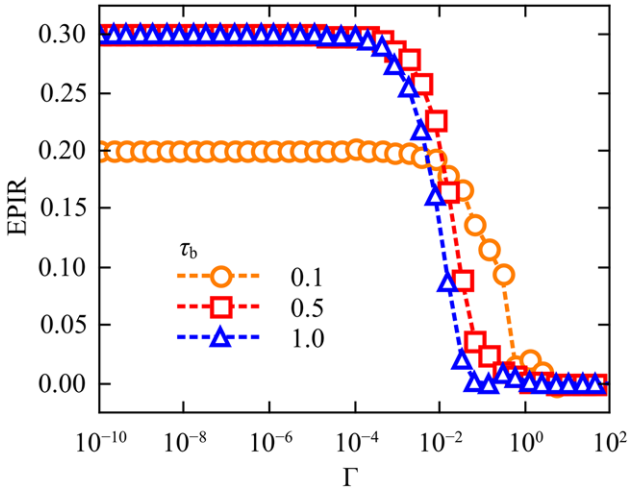

Figure 5. EPIR ratio as a function of external noise intensity for $\delta R = 3/4$ and $x(0) = 0.9$. Results correspond to the average of 1000 realizations.

An analytic expression for the probability distribution of $x(\tau)$ in equation (15) can be found. Indeed, it is easy to see that $x(\tau)$ in equation (15) must satisfy equations (3) and (5) where $g(\tau)$ is re-defined as

$$g(\tau) = \frac{x(0)}{(1-x(0))^{1/\beta}} \exp\left\{4\int_0^\tau (v(t)+\eta(t))\mathrm{d}t\right\}. \tag{16}$$

Let us call $y(\tau)$ the integral in the exponential. Since $y(\tau)$ is normal with mean $v(\tau)$ and variance $\Gamma\tau$, its probability density function, $f(y,\tau)$, is well known. From equation (3), we can write $y(\tau)$ as

$$y(\tau) = \log\left((1-x)^{-\frac{1}{4\beta}}x^{\frac{1}{4}}\right) - \log\left((1-x(0))^{-\frac{1}{4\beta}}x(0)^{\frac{1}{4}}\right).$$

Calling $F_{y(\tau)}$ and $F_{x(\tau)}$ the cumulative distribution functions of $y(\tau)$ and $x(\tau)$, respectively, then

$$F_{x(\tau)}(x) = F_{y(\tau)}\left(\log\left((1-x)^{-\frac{1}{4\beta}}x^{\frac{1}{4}}\right) - \log\left((1-x(0))^{-\frac{1}{4\beta}}x(0)^{\frac{1}{4}}\right)\right), \tag{17}$$

where we assumed a deterministic initial condition $x(0)$. Taking the derivative with respect to x, we find the probability density for $x(\tau)$

$$P(x,\tau) = f\left(\log\left[\left(\frac{1-x}{1-x(0)}\right)^{-\frac{1}{4\beta}}\left(\frac{x}{x(0)}\right)^{\frac{1}{4}}\right],\tau\right)\frac{1-\delta R\ x}{4x(1-x)}. \tag{18}$$

Figures 6 and 7 show the probability distributions of $x(\tau_b)$ (after the $+1$ pulse) and $x(2\tau_b)$ (after the -1 pulse), respectively. The initial condition is $x(0) = 0.5$, and $\delta R = 3/4$. As expected, the distribution broadens as Γ increases. Moreover, for high noise intensities, $\langle x(\tau_b)\rangle \approx \langle x(2\tau_b)\rangle \approx 0.5$ and, therefore, the EPIR ratio is approximately zero. The behavior of the EPIR ratio for other noise intensities can be understood by

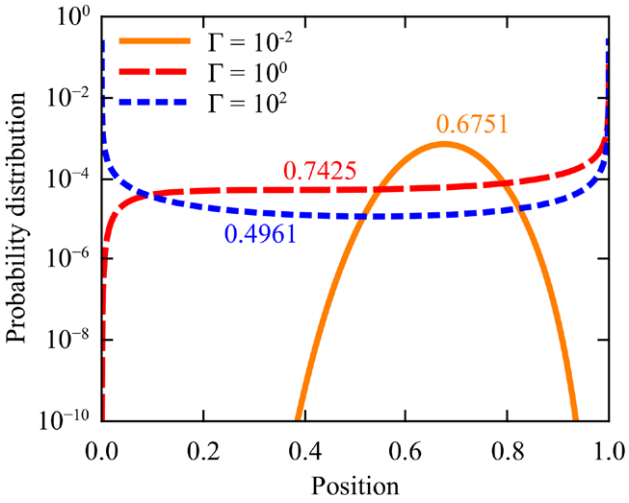

Figure 6. Probability distribution of $x(\tau_b)$ for $\delta R = 3/4$, $x(0) = 0.5$ and several values of external noise intensity. The corresponding mean values are shown next to each distribution.

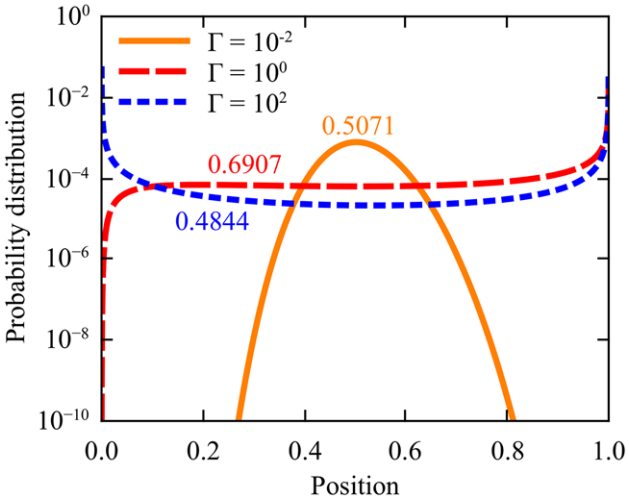

Figure 7. Probability distribution of $x(2\tau_b)$ for $\delta R = 3/4$, $x(0) = 0.5$ and several values of external noise intensity. The corresponding mean values are shown next to each distribution.

observing the distributions corresponding to $\Gamma = 1$ in figures 6 and 7. Note that, in this case, $\langle x(2\tau_b)\rangle \approx 0.7$. The state variable x does not 'return' to its initial condition $x(0) = 0.5$. The excursion of x values is smaller than that in the deterministic case and, thus, the EPIR ratio decreases. We must observe that, although the probability distributions seem to attain a non-zero value at the borders $x = 0$ and $x = 1$ for some values of the noise intensity, this is only an effect due to the resolution of the numerical data, as the probability distributions drop abruptly to zero. Indeed, from equation (15) the rate of change of the state variable tends to zero as it approaches either 0 or 1, and these values cannot be attained.

Let us now go back to equation (18). The probability density function is a product of two factors. It is not difficult to see that, for all $\delta R \in (0, 1)$, the second factor is a

concave function for $x \in (0,1)$ and it grows unbounded when $x \to 0,1$. Therefore, if the density function has a maximum in that interval, it has to be provided by the first factor. However, when the product $\Gamma\tau$ is large, the first factor becomes nearly constant and, thus, we observe a bathtub shape for $\Gamma = 0.2$ in figures 6–7. Only when the product $\Gamma\tau$ is small does the influence of the first factor become relevant, and the density exhibits a maximum approximately close to the position predicted by the deterministic equations (3)–(5) (see the curves for $\Gamma = 0.01$ in figures 6–7). For intermediate values of $\Gamma\tau$, but τ large enough for the deterministic predictions that $x(\tau)$ would be close to either 0 or 1, the decreasing tail of the first factor tends to compensate the growth of the second factor when x tends to 1 or 0, respectively. Indeed, this behavior is observed for $\Gamma = 1$ in figures 6–7. From the application point of view, we conclude that memory in a memristor is lost whenever $\Gamma\tau \gg 1$. In this sense, strong and short is more convenient than weak and long pulsing. Also, if external noise is present even in the absence of input, we can make a rough estimation of the memory persistence time as $T \sim \Gamma^{-1}$.

We must note that the effect of external noise in a memristor may probably be considered viewed as a problem of dithering, with the state variable $x(\tau)$ taken as the output signal and the driving voltage $v(\tau)$ as the input. In this sense, further insight might be obtained by resorting to the techniques described in [12].

5. Conclusions

We introduced a Fokker–Planck approach to tackle the effect of internal and external noise on resistive switching. In the case of internal noise, we resorted to a Fokker–Planck approach to account for the enhancement of the resistive contrast found in numerical simulations with non-harmonic driving signals. In the context of resistive memory devices, results suggest that internal noise may be advantageous for short driving pulses, i.e. as in the case for high-bandwidth devices.

When exploring the effect of external noise, and by analyzing the probability density function of the state variable, we found that noise only has the effect of degrading the resistive contrast, and obtained a relationship between the noise amplitude and the pulsewidth of the driving signal that constrains the persistence of the resistive state. In particular, results suggest that strong and short driving pulses favor a longer persistence time, an observation that may find applications in the field of high-integration high-speed resistive memory devices.

Although it may seem that internal and external noise are introduced into the equations almost in the same way, there is a substantial difference between them. While internal noise acts additively, external noise acts multiplicatively. It is a well-known fact that multiplicative and additive noise terms have very dissimilar effects (see, e.g. [13]).

Finally, it is important to point out that there exists experimental evidence of external noise enhancing the resistive contrast [4–6]. As we have shown, the model in equations (1)–(2) cannot account for such behavior. Although some work has been done towards a qualitative understanding based on phenomenological models (see [5]), we still lack a good quantitative explanation. Changes of electrical resistance are

commonly associated with the assisted migration of ions, such as oxygen vacancies. In this sense, a better explanation of the observed behavior might be found by analyzing the influence of external noise on ion migration models found in the literature (see, e.g. [14, 15]). Such an analysis remains a matter of future work.

Acknowledgment

We gratefully acknowledge financial support from ANPCyT under project PICT-2010 # 121.

References

[1] Chua L O 1971 Memristor-the missing circuit element *IEEE Trans. Circuit Theory* **18** 507–19
[2] Stotland A and Ventra M D 2012 Stochastic memory: memory enhancement due to noise *Phys. Rev.* E **85** 011116
[3] Patterson G A, Fierens P I and Grosz D F 2014 Resistive switching assisted by noise *Int. Conf. on Theory and Application in Nonlinear Dynamics (Understanding Complex Systems)* ed V In *et al* (Berlin: Springer) pp 305–11
[4] Patterson G A, Fierens P I, García A A and Grosz D F 2013 Numerical and experimental study of stochastic resistive switching *Phys. Rev.* E **87** 012128
[5] Patterson G A, Fierens P I and Grosz D F 2013 On the beneficial role of noise in resistive switching *Appl. Phys. Lett.* **103** 074102
[6] Patterson G A, Jimka F S, Fierens P I and Grosz D F 2015 Memristors under the influence of noise and temperature *Phys. Status Solidi* c **12** 187–91
[7] Strukov D B, Snider G S, Stewart D R and Williams R S 2008 The missing memristor found *Nature* **453** 80–3
[8] Slipko V A, Pershin Y V and Ventra M D 2013 Changing the state of a memristive system with white noise *Phys. Rev.* E **87** 042103
[9] Cai W, Ellinger F, Tetzlaff R and Schmidt T 2011 Abel dynamics of titanium dioxide memristor based on nonlinear ionic drift model arXiv:1105.2668
[10] Biolek Z, Biolek D and Biolkova V 2012 Analytical solution of circuits employing voltage- and current-excited memristors *IEEE Trans. Circuits Syst. I* **59** 2619–28
[11] Gardiner C 2009 *Stochastic Methods: a Handbook for the Natural and Social Sciences* (Berlin: Springer)
[12] Dimian M and Andrei P 2014 *Noise-Driven Phenomena in Hysteretic Systems* (New York: Springer)
[13] García-Ojalvo J and Sancho J 1999 *Noise in Spatially Extended Systems* (New York: Springer)
[14] Rozenberg M J, Sánchez M J, Weht R, Acha C, Gomez-Marlasca F and Levy P 2010 Mechanism for bipolar resistive switching in transition-metal oxides *Phys. Rev.* B **81** 115101
[15] Savel'ev S E, Alexandrov A S, Bratkovsky A M and Williams R S 2011 Molecular dynamics simulations of oxide memory resistors (memristors) *Nanotechnology* **22** 254011